

Low and Intermediate Re Solution of Lid Driven Cavity Problem by Local Radial Basis Function Collocation Method

K. Mramor¹, R. Vertnik^{2,3}, B. Šarler^{1,3,4,5}

Abstract: This paper explores the application of Local Radial Basis Function Collocation Method (LRBFCM) [Šarler and Vertnik (2006)] for solution of Newtonian incompressible 2D fluid flow for a lid driven cavity problem [Ghia, Ghia, and Shin (1982)] in primitive variables. The involved velocity and pressure fields are represented on overlapping five-noded sub-domains through collocation by using Radial Basis Functions (RBF). The required first and second derivatives of the fields are calculated from the respective derivatives of the RBF's. The momentum equation is solved through explicit time stepping. The method is alternatively structured with multiquadrics and inverse multiquadrics RBF's. In addition, two different approaches are used for pressure velocity coupling (Fractional Step Method (FSM) [Chorin (1968)] and Artificial Compressibility Method (ACM) [Chorin (1967)] with Characteristic Based Split (CBS) [Zienkiewicz and Codina (1995); Zienkiewicz, Morgan, Sai, Codina and Vasquez (1995)]). The method is tested for several low and intermediate Reynolds numbers (100, 400, 1000 and 3200) and node arrangements (41x41, 81x81, 101x101, 129x129). The original contribution of the paper represents extension of the LRBFCM to Reynolds number beyond 400 and assessment of the method for two different types of RBFs and two different types of pressure-velocity couplings. The obtained numerical results, in terms of mid-plane velocities, are in a good agreement with the data calculated in several reference publications and by commercial code. Both RBF's used give approximately the same results. Both pressure-velocity coupling methods give approximately the same results, however the FSM turns out to be slightly more efficient. The advantages of the method are simplicity, accuracy and straightforward applicability in non-uniform node arrangements.

¹ COBIK, Solkan, Slovenia.

² Štore Steel, Štore, Slovenia.

³ University of Nova Gorica, Nova Gorica, Slovenia.

⁴ Institute of Metals and Technology, Ljubljana, Slovenia.

⁵ Corresponding author: Professor Božidar Šarler, email: bozidar.sarler@ung.si

Keywords: 2D lid driven cavity, incompressible Newtonian fluid, meshless method, local radial basis function collocation method, fractional step method, artificial compressibility method with characteristic based split, multiquadrics, inverse multiquadrics

1 Introduction

Two-dimensional lid driven cavity flow problem is a widely studied benchmark case in the field of computational fluid dynamics (CFD) and has been traditionally used to study the accuracy and efficiency of various numerical methods. This benchmark test was first suggested by [Ghia, Ghia and Shin (1982)]. It describes a laminar incompressible Newtonian flow in a square cavity with moving top side and remaining walls fixed. The fluid inside the square cavity is set into motion by a moving upper wall. If the wall moves from the left to the right a clockwise rotating primary vortex is formed. By increasing the Re number, a hierarchy of eddies develops. The primary eddy is located at approximately the geometric center of the cavity whereas the higher order, smaller eddies, develop at top left and bottom left and right corners of the cavity and rotate in the opposite direction of the primary. The solutions are presented for various Reynolds (Re) numbers [Bruneau and Saad (2006); Erturk (2009)] and are for low Re almost identically confirmed by many authors [Botella and Peyret (1998); Erturk, Corke and Gökçöl (2005)]. Higher Re numbers (Re = 3200 and more), on the other hand, produce a much higher spread of the result [Erturk and Gökçöl (2006)], especially on coarser node arrangements. The test belongs to a spectrum of classical numerical benchmarks for assessment of numerical methods used in simulation of materials processing operations involving fluid flow. Complementary tests, which belong to the same category of important tests, are the natural convection benchmark [De Vahl Davis (1983)], freezing with natural convection benchmark [Gobin and Le Quéré (2000)], and very recent binary solidification benchmark [Bellet, Combeau, Fautrelle, Gobin, Rady, Arquis, Budenkova, Dussoubs, Duterrail, Kumar, Gandin, Goyeau, Mosbah and Zaloznik (2009)].

A wide variety of different numerical methods have already been applied for the driven cavity problem. Among them are the Finite Difference Method (FDM) [Bruneau and Jouron (1990), Bruneau and Saad (2006)], the Finite Element Method (FEM) [Barragy and Carey (1997)], different variations of Boundary Element Method (BEM) [Liao (1992); Liao and Zhu (1996); Grigoriev and Dargush (1999); Aydin and Fenner (2001)], the Chebyshev Collocation Method (CCM) [Botella and Peyret (1998)], the Multi Grid Method (MGM) [Ghia, Ghia, and Shin (1982)], the Lattice Boltzman Method (LBM) [Hou, Zou, Chen, Doolen and Cogley (1995)], and many others.

In the last decade, meshless numerical methods [Atluri and Shen (2002); Atluri (2004); Gu and Liu (2005); Fasshauer (2007); Liu (2010)] started to represent an appealing alternative to the classical numerical methods. Meshless method is a numerical technique that uses a set of arbitrary distributed nodes, both on the boundary and within the computation domain, to represent the solution of physical phenomena. The main feature of meshless methods is omission of the polygonalisation between the nodes which can be remarkably demanding, particularly in realistic 3D geometrical situations. One of the simplest meshless methods, able to solve the fluid flow problems [Šarler, Perko and Chen (2004); Šarler (2005)] is the Radial Basis Function Collocation Method (RBFCM) [Kansa (1990a,b)]. In this paper, its Local version (LRBFCM) [Šarler and Vertnik (2006)] is focused. The idea behind this method is to approximate the function locally over a set of neighboring nodes using RBFs [Buhmann (2000)] and to use collocation for determining the expansion coefficients.

Respectively, the focused lid driven cavity problem was already solved by several meshless methods, such as the Meshless Local Petrov-Galerkin (MLPG) method [Lin and Atluri (2001)] for $Re = 100$ and $Re = 400$, the Method of Fundamental Solutions (MFS) [Young, Jane, Fan, Murugesan and Tsai (2006)] for $Re = 100$ and $Re = 400$, the Meshfree Point Collocation method (MPC) [Kim, Kim, Jun and Lee (2007)] for $Re = 100, 400$ and 1000 , and the LRBFCM [Divo and Kassab (2007)] implemented for $Re = 100$ and 400 . The LRBFCM method was first developed by [Tolstykh and Shirobokov (2003)] for elasticity problems and [Šarler and Vertnik (2006)] for diffusion problems. Since then, it has been successfully applied to various academic and industrial cases involving fluid flow. In [Kosec and Šarler (2008a)], classical De Vahl Davis natural convection benchmark and natural convection in Darcy porous media [Kosec and Šarler (2008b)] have been solved by employing completely local pressure correction. The extensions of the method to melting and freezing with natural convection have been described in [Kosec and Šarler (2009), Kosec and Šarler (2010)]. The macrosegregation phenomena have been for the first time solved by LRBFCM in [Kosec, Založnik, Šarler and Combeau (2011)], where the authors for the first time demonstrate discretization independent results for this extremely non-linear coupled problem. The low Pr natural convection was considered in [Kosec and Šarler (2013)]. In [Vertnik and Šarler (2009)], $k-\varepsilon$ model of the turbulence has been solved by LRBFCM, representing a pioneering solution of engineering description of turbulence by any of the meshless numerical methods. In [Vertnik and Šarler (2011)] turbulent forced and natural convection problems have been solved. R-adaptive and H-adaptive version of the method have been developed in [Kovačević and Šarler (2005)] and [Kosec and Šarler (2011)].

Recently, there is a strong development in the direction of combining meshless concepts, based on radial basis functions and finite volume concepts [An-Vo, Mai-Duy and Tran-Cong (2011a, b); An-Vo, Mai-Duy, Tran and Tran-Cong (2013)] as well as RBFs and finite difference concepts [Wright and Fornberg (2006); Bayona, Moscoso, Carretero and Kindelan (2010)]. Related efforts have been made also in the context of weak formulation by combining MLPG and the finite volume concepts [Avila, Han and Atluri (2011)].

In this paper, LRBFCM is tested on a lid driven cavity benchmark case, for low and intermediate Re, at four different node arrangements, varying from 1681 to 16641 nodes (41x41, 81x81, 101x101, 129x129), at four different Re (100, 400, 1000 and 3200), two different pressure velocity coupling approaches and two different RBF types. The results obtained are compared with the results from [Ghia, Ghia and Shin (1982); Bruneau and Jouron (1990); Botella and Peyret (1998); Sahin and Owens (2003a,b); Erturk, Corke and Gökçöl (2005)], and with the results of commercial code FLUENT [Fluent (2003)]. The motivation for the present paper is extension of the work of [Divo and Kassab (2007)] to intermediate Re numbers, and assessment of performance of different radial basis functions, and different pressure - velocity couplings for subsequent use in more involved materials processing simulations, such as continuous casting [Šarler, Vertnik and Mramor (2012)].

2 Governing equations and solution procedure

The Newtonian incompressible flow in fixed domain Ω with boundary Γ is described by the following Navier-Stokes equations

$$\rho \frac{\partial \mathbf{v}}{\partial t} + \rho \nabla \cdot (\mathbf{v}\mathbf{v}) = -\nabla p + \mu \nabla^2 \mathbf{v}, \quad (1)$$

$$\nabla \cdot \mathbf{v} = 0, \quad (2)$$

where \mathbf{v} stands for velocity vector, t is time, p pressure, ρ density and μ viscosity. The solution of mass (Eq. 2) and momentum (Eq. 1) equations (p, \mathbf{v}) is sought for velocity and pressure at time $t_0 + \Delta t$, where Δt represents a positive time increment, by assuming the known consistent velocity and pressure fields at initial time t_0 (p_0, \mathbf{v}_0), and specified Dirichlet boundary conditions applied on the boundary Γ for time $t > t_0$.

2.1 Solution procedure

The time discretization is performed with explicit Euler method. Further elements of the solution procedure are explained in continuum setting, where no reference has to be made with respect to space discretization. The elements of the local

meshless method, used for space discretization are explained in Section 2.3. The solution procedure is structured as follows. First, the intermediate velocity \mathbf{v}^* at $t_0 + \Delta t$ is calculated from the momentum equation, without the pressure gradient

$$\mathbf{v}^* = \mathbf{v}_0 + \frac{\Delta t}{\rho} [-\rho \nabla \cdot (\mathbf{v}\mathbf{v}) + \mu \nabla^2 \mathbf{v}]_0. \quad (3)$$

Subsequently, two different approaches for pressure velocity coupling are used in the present work: Fractional Step Method (FSM) [Chorin (1968)] and Artificial Compressibility Method (ACM) [Chorin (1967)] with Characteristic Based Split (CBS) [Zienkiewicz and Codina (1995); Zienkiewicz, Morgan, Sai, Codina and Vasquez (1995)]. In both methods, the velocity components are corrected by the pressure gradient

$$\mathbf{v} = \mathbf{v}^* - \frac{\Delta t}{\rho} \nabla p. \quad (4)$$

The related pressure is calculated either with FSM or ACM with CBS, both of which are described below.

2.2 FSM and ACM with CBS pressure velocity-coupling

In FSM method, the pressure is calculated from Poisson's equation

$$\nabla^2 p = \frac{\rho}{\Delta t} \nabla \cdot \mathbf{v}^*, \quad (5)$$

with Neumann boundary conditions

$$\frac{\partial p}{\partial \mathbf{n}} = 0. \quad (6)$$

In ACM method, the pressure field is obtained from the following equation

$$p = p_0 - \beta^2 \Delta t (\rho \nabla \cdot \mathbf{v}^* - \Delta t \nabla^2 p_0), \quad (7)$$

where $-\Delta t \nabla^2 p_0$ is a stabilization term as applied in the CBS, and β is the compressibility coefficient. The selection of optimum compressibility coefficient is problem dependent. A more detailed description of the FSM method can be found in [Chorin, (1968)], and ACM method is elaborated in [Chorin (1967)], and in the articles of [Zienkiewicz and Codina (1995); Zienkiewicz, Morgan, Sai, Codina, and Vasquez (1995)] where CBS term is added.

Finally, the velocity and pressure are updated ($\mathbf{v} = \mathbf{v}_0$, $p = p_0$) and the solution is ready for the next step. The steady state is reached when the following criteria is satisfied in each of the N computational nodes

$$|\mathbf{v}_i - \mathbf{v}_{i0}| < \varepsilon_v, \quad |p_i - p_{i0}| < \varepsilon_p, \quad i = 1, \dots, N, \quad (8)$$

where ε_v , and ε_p are the velocity and pressure iteration criteria, respectively.

2.3 Local radial basis function collocation method

In the LRBFCM, a set of RBF interpolation functions and collocation are used to solve partial differential equations (PDEs). The method is implemented locally on a set of neighboring nodes that can be uniformly or non-uniformly arranged. The region consists of N calculation points, of which there are N_Ω domain and N_Γ boundary points, and it is divided into N overlapping subdomains, each of which consists of ${}_l M$ (in general) non-equally spaced nodes ${}_l \mathbf{p}_n$, where $l = 1, \dots, N$ stands for subdomain and $n = 1, \dots, {}_l M$ is the number of subdomain nodes (see Fig. 1).

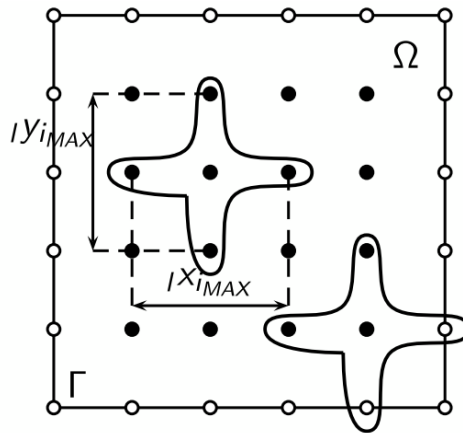


Figure 1: Scheme of the discretization. The Γ , Ω , ${}_l X_{iMAX}$, ${}_l Y_{iMAX}$ represent boundary, domain and scaling parameters in x and y direction respectively. Empty dots represent boundary nodes whereas black dots represent domain nodes (see [Mramor, Vertnik and Šarler (2013)]).

On each of the N subdomains, function θ is expressed with RBFs as

$$\theta(\mathbf{p}) \approx \sum_{i=1}^M {}_l \psi_i(\mathbf{p}) {}_l \gamma_i, \quad (9)$$

where \mathbf{p} stands for a position vector, ${}_l \psi_i$ are a set of RBFs centered in points ${}_l \mathbf{p}_i$, ${}_l \gamma_i$ are the expansion coefficients and M is the number of shape functions. In the present paper, overlapping five-noded subdomains are used. The LRBFCM is in the present work implemented with multiquadric (MQ) and inverse multiquadric (IMQ) RBF shape functions [Franke (1982)]

$${}_l \psi_{iMQ}(\mathbf{p}) = \sqrt{{}_l r_i^2 + c^2}, \quad {}_l \psi_{iIMQ}(\mathbf{p}) = \frac{1}{\sqrt{{}_l r_i^2 + c^2}}, \quad (10)$$

where c stands for dimensionless shape parameter, which is predetermined, and ${}_l r_i$ is

$${}_l r_i(\mathbf{p}) = \sqrt{\left(\frac{x-x_i}{x_{iMAX}}\right)^2 + \left(\frac{y-y_i}{y_{iMAX}}\right)^2 + c^2}, \quad (11)$$

where ${}_l x_{iMAX}$, and ${}_l y_{iMAX}$ stand for a maximum distance in x and y direction in sub-domain l , respectively. In order to determine the coefficients, the collocation

$$\theta({}_l \mathbf{p}_n) = {}_l \theta_n = \sum_{i=1}^M {}_l \psi_i({}_l \mathbf{p}_n) {}_l \gamma_i, \quad (12)$$

is used. A linear system of M equations is obtained from Eq. 12

$${}_l \boldsymbol{\Psi} {}_l \boldsymbol{\gamma} = {}_l \boldsymbol{\theta}, \quad (13)$$

where the components of interpolation matrix ${}_l \boldsymbol{\Psi}$ are RBFs. In case, when the number of domain nodes ${}_l M$ matches the number of the basis functions M and when the basis functions matrix is non-singular [Hon and Schaback (2001)], the expansion coefficients can be computed from

$${}_l \boldsymbol{\gamma} = {}_l \boldsymbol{\Psi}_l^{-1} {}_l \boldsymbol{\theta}. \quad (14)$$

$\theta(\mathbf{p})$ can afterwards be approximately expressed as

$$\theta(\mathbf{p}) \approx \sum_{n=1}^M {}_l \psi_i(\mathbf{p}) \sum_{k=1}^M {}_l \psi_{ik}^{-1}(\mathbf{p}) {}_l \theta_k. \quad (15)$$

In order to be able to solve the PDEs, the first and the second derivative of function $\theta(\mathbf{p})$ have to be calculated on the influence domain. The operator applied on the approximation function is expressed by [Kansa (1990a,b)]

$$\frac{\partial^j}{\partial \chi^j} {}_l \theta(\mathbf{p}) = \sum_{i=1}^M {}_l \gamma_i \frac{\partial^j}{\partial \chi^j} {}_l \psi_i(\mathbf{p}), \quad (16)$$

where the index j is used to denote the order of derivative and $\chi = x, y$. The first and the second derivatives of MQ in 2D are

$$\begin{aligned} \frac{\partial \psi_{iMQ}}{\partial x} &= \frac{x-x_i}{x_{iMAX}^2} (r_i^2 + c^2)^{-\frac{1}{2}}, \\ \frac{\partial \psi_{iMQ}}{\partial y} &= \frac{y-y_i}{y_{iMAX}^2} (r_i^2 + c^2)^{-\frac{1}{2}}, \\ \frac{\partial^2 \psi_{iMQ}}{\partial x^2} &= \frac{1}{x_{iMAX}^2} (r_i^2 + c^2)^{-\frac{1}{2}} - \frac{x-x_i}{x_{iMAX}^2} (r_i^2 + c^2)^{-\frac{3}{2}}, \\ \frac{\partial^2 \psi_{iMQ}}{\partial x \partial y} &= -\frac{x-x_i}{x_{iMAX}^2} \frac{y-y_i}{y_{iMAX}^2} (r_i^2 + c^2)^{-\frac{3}{2}}, \\ \frac{\partial^2 \psi_{iMQ}}{\partial y^2} &= \frac{1}{y_{iMAX}^2} (r_i^2 + c^2)^{-\frac{1}{2}} - \frac{y-y_i}{y_{iMAX}^2} (r_i^2 + c^2)^{-\frac{3}{2}}, \end{aligned} \quad (17)$$

and of IMQ in 2D are

$$\begin{aligned}
 \frac{\partial \psi_{iIMQ}}{\partial x} &= \frac{x-x_i}{x_{iMAX}^2} (r_i^2 + c^2)^{-\frac{3}{2}}, \\
 \frac{\partial \psi_{iIMQ}}{\partial y} &= \frac{y-y_i}{y_{iMAX}^2} (r_i^2 + c^2)^{-\frac{3}{2}}, \\
 \frac{\partial^2 \psi_{iIMQ}}{\partial x^2} &= 3 \left(\frac{x-x_i}{x_{iMAX}^2} \right)^2 (r_i^2 + c^2)^{-\frac{5}{2}} - \frac{1}{y_{iMAX}^2} (r_i^2 + c^2)^{-\frac{3}{2}}, \\
 \frac{\partial^2 \psi_{iIMQ}}{\partial x \partial y} &= 3 \left(\frac{x-x_i}{x_{iMAX}^2} \right)^2 \left(\frac{y-y_i}{y_{iMAX}^2} \right)^2 (r_i^2 + c^2)^{-\frac{5}{2}} \\
 \frac{\partial^2 \psi_{iIMQ}}{\partial y^2} &= 3 \left(\frac{y-y_i}{y_{iMAX}^2} \right)^2 (r_i^2 + c^2)^{-\frac{5}{2}} - \frac{1}{x_{iMAX}^2} (r_i^2 + c^2)^{-\frac{3}{2}}.
 \end{aligned} \tag{18}$$

The ACM method uses local updating of the pressure, explained in Eq. 7 to solve the new pressure, whereas in the FSM method, the Poisson equation has to be solved globally. The solution of the Poisson equation leads to a sparse matrix, with a similar structure as introduced in [Lee, Liu and Fan (2003)] for solving boundary value problems. The local $l\mathbf{p}_n$ and global \mathbf{p}_k points in this case coincide and the relation between them is introduced as $\mathbf{p}_{k(l,n)} = l\mathbf{p}_n$. The pressure is represented on each of the subdomains by RBFs and their coefficients as

$$p(\mathbf{p}) = \sum_{n=1}^M \psi_{i(l,n)}(\mathbf{p}) l\gamma_n, \tag{19}$$

and $l\gamma$ is determined as presented in Eq. 14. The pressure is thus

$$p_{i(l,m)} = \sum_{n=1}^M l\Psi_{mn} l\gamma_n; \quad m = 1, \dots, M, \tag{20}$$

and can be calculated in each of the subdomains as

$$p(\mathbf{p}) = \sum_{n=1}^M \sum_{m=1}^M l\psi_{i(l,n)}(\mathbf{p}) l\Psi_{nm}^{-1} p_{i(l,m)}. \tag{21}$$

The collocation in global point \mathbf{p}_k is finally expressed in a form

$$\sum_{j=1}^N \Psi_{kj} \mathbf{p}_j = S_k; \quad k = 1, 2, \dots, N, \tag{22}$$

where Ψ_{kj} is the global sparse matrix element.

2.4 Numerical implementation

The method has been numerically implemented with solver coded in Fortran and executed on 2 Intel Xeon processors with 8 2.0 GHz cores with 64 bit Windows 8

server operating system. The ACM with CBS pressure velocity coupling procedure is solved locally with LRBFCM. The sparse matrix obtained in FSM for the solution of Poisson equation (Eq. 5) is solved in global points with Pardiso routine and Intel Math Kernel Library 11. OpenMP is used for parallelization and Gnuplot 4.4. is used for post-processing.

3 Numerical examples

The problem is solved on a fixed square domain $\Omega = [0,1] \times [0,1]$ with boundary Γ , where Dirichlet boundary conditions are applied on all walls. Cartesian coordinate system is used ($\mathbf{p} = (p_x, p_y)$). The velocity ($\mathbf{v} = (v_x, v_y)$) is zero for stationary walls (left, right and bottom) and have the value of $v_x=1$ m/s and $v_y=0$ for the top moving wall. Eq. 1 and 2 are in their dimensionless form written as follows

$$\frac{\partial \mathbf{v}'}{\partial t'} + \mathbf{v}' \cdot \nabla' \mathbf{v}' = -\nabla' p' + \frac{1}{\text{Re}} \nabla'^2 \mathbf{v}', \quad \nabla' \cdot \mathbf{v}' = 0, \quad (23)$$

where \mathbf{v}' , t' , p' are dimensionless velocity, time and pressure and Re is Reynolds number, defined as

$$\mathbf{v}' = \frac{\mathbf{v}}{v_\ell}, \quad t' = \frac{t v_\ell}{\ell}, \quad p' = \frac{p}{\rho v_\ell^2}, \quad \text{Re} = \frac{v_\ell \ell}{\nu}, \quad (24)$$

where $\ell=1$ m stands for characteristic dimension and equals the length of the side of the cavity L , $v_\ell=1$ m/s is the characteristic velocity and $\nu = \mu/\rho$ is the dynamic viscosity.

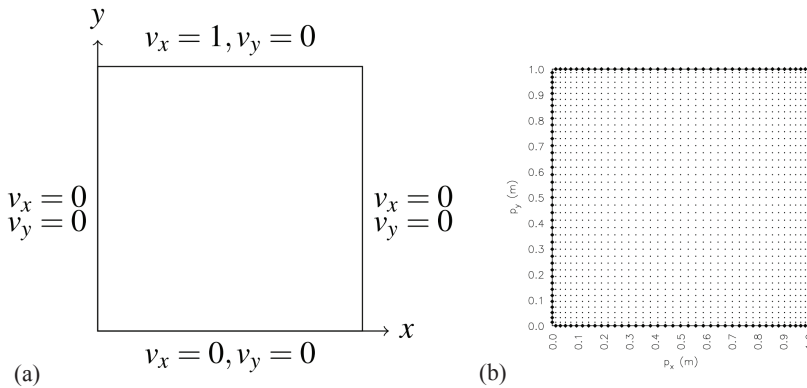


Figure 2: Scheme of the computational domain of a two-dimensional cavity. (a) boundary conditions, and (b) node arrangement (41 x 41, b=1.2).

The solution of the problem $\mathbf{v}'(\mathbf{p})$, $p'(\mathbf{p})$ with initial conditions $\mathbf{v}'_0 = 0$ and $p'_0 = 0$, is sought. The scheme of the problem with boundary conditions is depicted in Fig. 2.

The numerical examples are organized in the following way: (I) the convergence of the method is investigated for different node arrangements, (II) the results are compared with the results obtained by other authors, (III) the comparison of different RBF types is checked and lastly (IV) a comparison between two different pressure velocity couplings is made. All of the calculations are done for $c=32$. The time step $\Delta t'$ used is 10^{-3} . The velocity and pressure iteration criteria are set to 10^{-5} . Unless otherwise stated, the calculations were done with MQ and FSM pressure velocity coupling scheme.

3.1 Convergence of the method

The convergence of the method was investigated for $Re = 1000$ and four node arrangements, varied between 1681 nodes (41×41) and 16641 (129×129) nodes. The velocities were compared along vertical and horizontal lines through geometric center of the cavity. The comparisons are shown in Fig. 3. As expected, the node arrangement with the smallest number of nodes gives slightly poorer results. The velocity profiles of the denser node arrangements are almost the same and are in accordance with the expected velocity profiles.

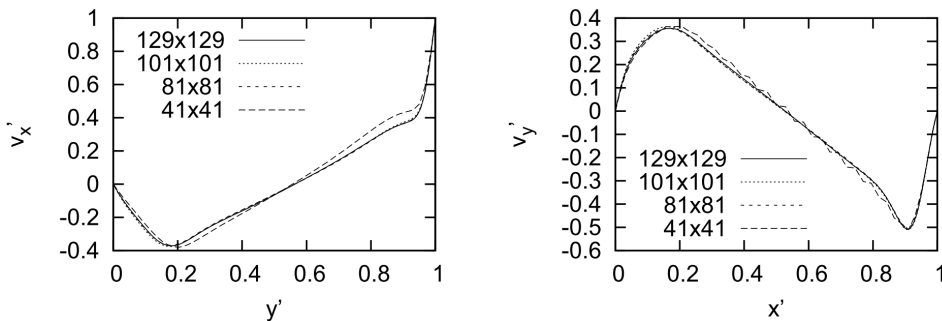


Figure 3: Comparison of velocities for different node densities for $Re=1000$. Left: v'_x component of velocity along horizontal line through the center of the cavity. Right: v'_y component of velocity along the vertical line through the center of the cavity.

3.2 Comparison with reference results

Lid driven cavity flow was calculated for low to intermediate Re, ranging between 100 and 3200. The results, obtained with 81 x 81 node arrangement are shown in Figs. 4-7. The velocities are compared to the spectra of results, given by [Ghia, Ghia and Shin (1982); Erturk, Corke and Gökçöl (2005); Botella and Peyret (1998); Sahin and Owens (2003a,b); Bruneau and Jouron (1990)]. As expected, the best agreement between the calculated and the previously published velocity profiles is achieved for small Re (100 and 400). The agreement between data and calculations is slightly poorer for intermediate Re (1000 and 3200), which is expected as the flow is more structured and a larger number of nodes is needed to get a reasonable approximation. The odd data point in the right graph in Fig. 5 is probably a wrongly entered number in the table to [Ghia, Ghia and Shin (1982)]. Additionally, for Re = 400, the velocity profiles are also compared to the results obtained with FLUENT code.

The minimum (for v'_x and v'_y) and the maximum (for v'_y) values of velocities along horizontal and vertical lines that pass through the geometric center of the cavity are given in Tab. 1 for 129 x 129 node arrangement for a variety of different Re.

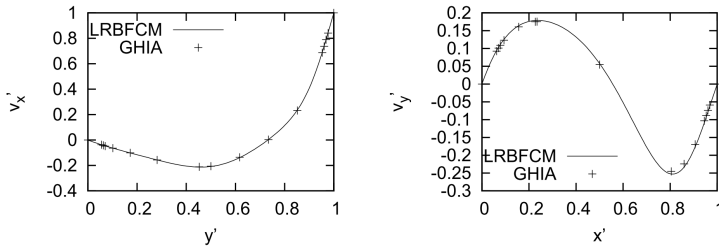


Figure 4: Comparison of velocities for Re=100, calculated with LRBFCM and results by [Ghia, Ghia & Shin (1982)]. Left: v'_x component of velocity along horizontal line through the center of the cavity. Right: v'_y component of velocity along the vertical line through the center of the cavity.

3.3 Comparison of MQ and IMQ RBF types

A comparison between two different RBF types was done for Re = 1000. As can be seen in Fig. 8, the results are almost the same (minimum velocities in x direction are -0.3674 (IMQ) and -0.3713 (MQ), and in y direction -0.5035 (IMQ) and -0.5082 (MQ)) for both types of RBF. The number of iterations to achieve the steady state is the same and the CPU time for IMQ is slightly higher due to slightly more complicated algebraic expressions.

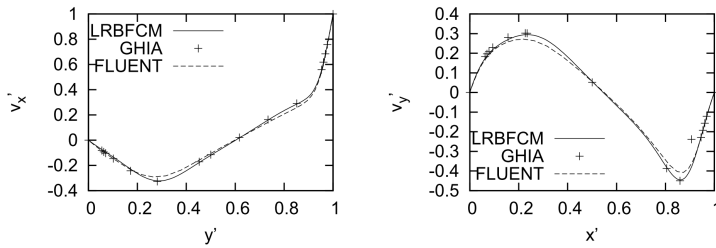


Figure 5: Comparison of velocities for $Re = 400$, calculated with LRBFCM and results by [Ghia, Ghia & Shin (1982)]. Left: v'_x component of velocity along horizontal line through the center of the cavity. Right: v'_y component of velocity along the vertical line through the center of the cavity.

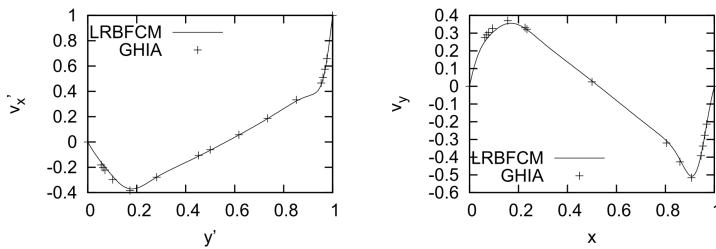


Figure 6: Comparison of velocities for $Re = 1000$, calculated with LRBFCM and results by [Ghia, Ghia & Shin (1982)]. Left: v'_x component of velocity along horizontal line through the center of the cavity. Right: v'_y component of velocity along the vertical line through the center of the cavity.

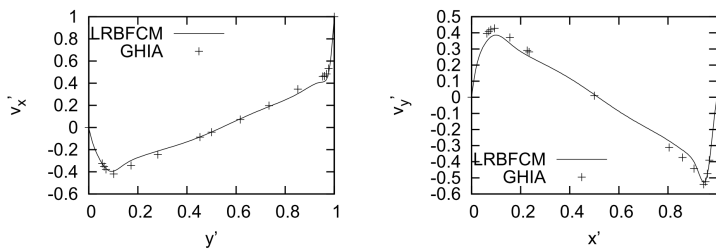


Figure 7: Comparison of velocities for $Re = 3200$, calculated with LRBFCM and results by [Ghia, Ghia & Shin (1982)]. Left: v'_x component of velocity along horizontal line through the center of the cavity. Right: v'_y component of velocity along the vertical line through the center of the cavity.

Table 1: Minimum and maximum velocities along horizontal line ($y=0.5$) and vertical line ($x=0.5$) through the center of the cavity for different Re. 1: present, 2: [Ghia, Ghia, and Shin (1982)], 3: [Erturk, Corke and Gökçöl (2005)], 4: [Botella and Peyret (1998)], 5: [Sahin and Owens (2003a)], 6: [Bruneau and Jouron (1990)].

Re	v'_x (min)	y	v'_y (min)	x	v'_y (max)	x	Ref.
100	-0.21325	0.4542	-0.25296	0.8102	0.17884	0.2379	1
	-0.21090	0.4531	-0.24533	0.8047	0.17527	0.2344	2
	-0.21392	0.4598	-0.25660	0.8127	0.18089	0.2354	5
	-0.2106	0.4531	-0.2521	0.8125	0.1786	0.2344	6
400	-0.32276	0.2876	-0.44523	0.8637	0.29453	0.2379	1
	-0.32726	0.2813	-0.44993	0.8594	0.30203	0.2266	2
	-0.32838	0.2815	-0.45632	0.8621	0.30445	0.2253	5
1000	-0.37126	0.1820	-0.50821	0.9070	0.35603	0.1665	1
	-0.38289	0.1719	-0.51550	0.9063	0.37095	0.1563	2
	-0.38690	0.1800	-0.52630	0.9100	0.37560	0.1500	3
	-0.38866	0.1719	-0.52644	0.9063	0.37692	0.1563	4
	-0.38810	0.1727	-0.52845	0.9087	0.37691	0.1573	5
	-0.37640	0.1602	-0.5208	0.9102	0.3665	0.1523	6
3200	-0.39664	0.0930	-0.52900	0.94710	0.38611	0.1000	1
	-0.41933	0.1016	-0.54053	0.9453	0.42768	0.0938	2
	-0.43540	0.0921	-0.56915	0.9491	0.43245	0.0972	5

Table 2: Numerical examples for testing different RBFs with relevant parameters at Re = 1000 and 129 x 129 nodes.

case	RBF	iter.	CPU time [s]	v'_x (min)	v'_y (min)
1	MQ	20900	7825.88	-0.3713	-0.5082
2	IMQ	20900	9145.25	-0.3674	-0.5035

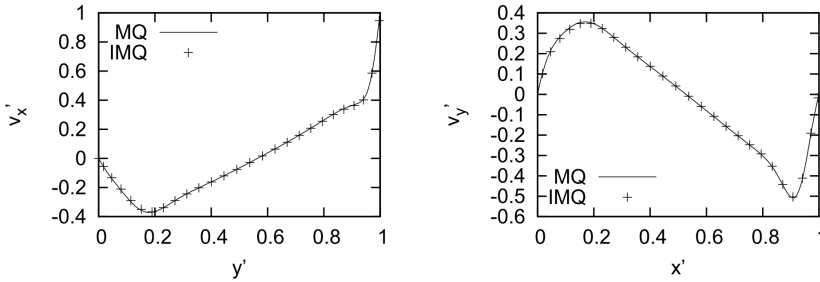


Figure 8: Comparison of two different RBF types (MQ and IMQ) (cases 1 and 2 in Tab. 2). Left: v'_x velocity along horizontal line through the center of the cavity. Right: v'_y velocity along the vertical line through the center of the cavity.

3.4 Comparison of two different pressure velocity coupling schemes

The difference between two different velocity pressure coupling methods is investigated for 129×129 node arrangement and $Re = 1000$. The first method is FSM and the second method is ACM with CBS term. The fixed compressibility coefficient used in ACM method is $\beta = 1$. The pressure, calculated with ACM with CBS term is calculated directly in each of the nodes. The selection of optimum β is not trivial. The FSM method, on the other hand, requires the calculation of a sparse matrix which is a much more involved operation as pointwise pressure calculation. The ACM with CBS term requires more iterations to reach the steady state. It turns out that FSM is faster and needs less iterations to reach the steady state, despite the need to calculate a sparse matrix, especially in cases with larger node arrangements. In our case, both of the methods give similar results, which are shown in Fig. 9. The CPU times and the number of iterations needed to reach the steady state are presented in Tab. 3.

Table 3: Sensitivity study with respect to different pressure velocity coupling at $Re = 1000$ and 129×129 nodes.

case	RBF	p-v coupling	iter.	CPU time [s]	v'_x (min)	v'_y (min)
1	MQ	FSM	20900	7825.88	-0.3713	-0.5082
3	MQ	ACM	31400	9951.03	-0.3780	-0.5080

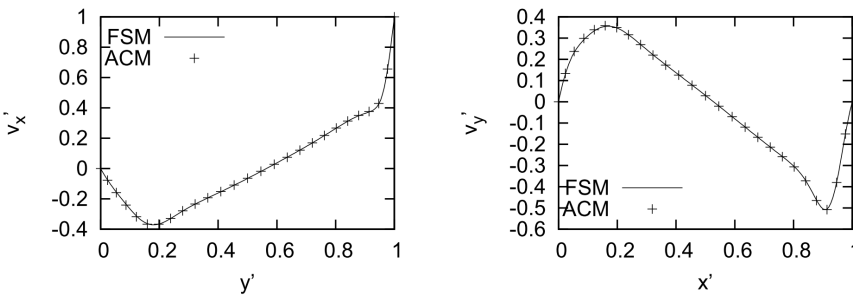
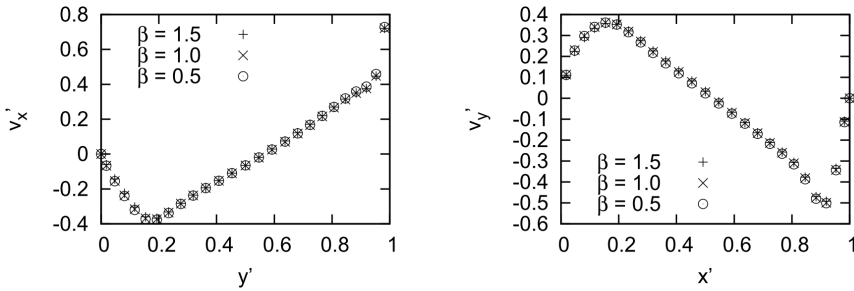


Figure 9: Comparison of velocities for different pressure velocity coupling methods (cases 1 and 3 in Tab. 3). Left: v'_x component of velocity along horizontal line through the center of the cavity.

In Tab. 4 a comparison of minimum velocities on centerlines as a function of β are presented. The minimum velocities are not sensitive to the choice of β (see also Fig.10), however, the largest β chosen in the study gives the most efficient solution.

Table 4: Sensitivity study with respect to compressibility coefficient at $Re = 1000$ and 129×129 nodes.

case	RBF	β	iter.	CPU time [s]	v'_x (min)	v'_y (min)
3b	MQ	0.5	72700	22597.94	-0.3809	-0.5116
3	MQ	1.0	31400	9951.03	-0.3780	-0.5080
3c	MQ	1.5	26400	6974.48	-0.3702	-0.5019

Figure 10: Comparison of velocities for different β (Tab. 4). Left: v'_x component of velocity along horizontal line through the center of the cavity. Right: v'_y component of velocity along the vertical line through the center of the cavity.

4 Conclusions

The LRBFCM method is applied to the driven cavity problem with Re that vary in the low and intermediate range, from 100 to 3200. The results are compared to the published results of several authors [Ghia, Ghia and Shin (1982); Bruneau and Jouron (1990); Botella and Peyret (1998); Sahin and Owens (2003a,b); Erturk, Corke and Gökçöl (2005)], and with the results, obtained with FLUENT commercial CFD package. The LRBFCM is for the first time applied on a lid driven cavity benchmark case with Re 1000 and above. The convergence is explored for several different node arrangements, ranging from 41×41 nodes to 129×129 nodes. The calculated results are in good agreement with the reference results. The study was made to test the efficiency and accuracy of the pressure-velocity coupling calculation schemes. Respectively, two different methods for pressure-velocity coupling are compared. Both, the FSM and ACM with CBS give similar results. However, the FSM method turns out to be slightly more efficient as it requires a lower number of iterations as well as CPU time to reach the steady state. The main advantage of LRBFCM is its accuracy, no need for polygonisation and a very simple numerical implementation on the non-uniform node arrangements. We will continue our

research of the problem by considering the high Re non-steady situations. In this case, the upwinding strategy, first proposed in connection with the meshless methods by Lin and Atluri [Lin and Atluri (2000)], will most probably have to be used.

Acknowledgement

The research in this paper was sponsored by Centre of Excellence for Biosensors, Instrumentation and Process Control (COBIK) and the Slovenian Grant Agency under grant J2-4120 and program P2-0379. COBIK is an operation financed by the European Union, European Regional Development Fund and Republic of Slovenia, Ministry of Education, Science, Culture and Sport.

References

- An-Vo, D.A.; Mai-Duy, N.; Tran-Cong, T.** (2011a): A C2-continuous control-volume technique based on Cartesian grids and two-node integrated RBF elements for second-order elliptic problems. *CMES: Computer Modeling in Engineering and Sciences*, vol. 72, pp. 299-335.
- An-Vo, D.A.; Mai-Duy, N.; Tran-Cong, T.** (2011b): High-order upwind methods based on C2-continuous two-node integrated-RBF elements for viscous flows. *CMES: Computer Modeling in Engineering and Sciences*, vol. 80, pp. 141-177.
- An-Vo, D.A.; Mai-Duy, N.; Tran, C.D.; Tran-Cong, T.** (2013): ADI method based on C2-continuous two-node integrated-RBF elements for viscous flow. *Applied Mathematical Modeling*, vol. 37, pp. 5184-5203.
- Atluri, S.N.; Shen, S.** (2002): *The Meshless Method*. Tech Science Press, Encino.
- Atluri, S.N.** (2004): *The Meshless Method (MLPG) for Domain and Boundary Discretizations*. Tech Science Press, Encino.
- Avila, R.; Han, Z.; Atluri, S.N.** (2011): A novel MLPG-finite-volume mixed method for analyzing Stokesian flows & study of a new vortex mixing flow. *CMES: Computer Modeling in Engineering & Sciences*, vol. 71, pp. 363-395.
- Aydin, M.; Fenner, R.** (2001): Boundary element analysis of driven cavity flow for low and moderate Reynolds numbers. *International Journal for Numerical Methods in Fluids*, vol. 37, pp. 45-64.
- Barragy, E.; Carey, G.** (1997): Stream function-vorticity driven cavity solution using finite elements. *Computers and Fluids*, vol. 26, pp. 453-468.
- Bayona, V.; Moscoso, M.; Carretero, M.; Kindelan, M.** (2010): RFB-FD formulas and convergence properties. *Journal of Computational Physics*, vol. 229, pp.8281-8295.

Bellet, M.; Combeau, H.; Fautrelle, Y.; Gobin, D.; Rady, M.; Arquis, E.; Budenkova, O.; Dussoubs, B.; Duterrail, Y.; Kumar, A.; Gandin, C. A.; Goyeau, B.; Mosbah, S.; Zaloznik, M. (2009): Call for contributions to a numerical benchmark problem for 2D columnar solidification of binary alloys. *International Journal of Thermal Sciences*, vol. 48, pp. 2013-2016.

Botella, O.; Peyret, R. (1998): Benchmark spectral results on the lid-driven cavity flow. *Computers and Fluids*, vol. 27, pp. 421-433.

Bruneau, C.; Jouron, C. (1990): An efficient scheme for solving steady incompressible Navier-Stokes equations. *Journal of Computational Physics*, vol. 89, pp. 389-413.

Bruneau, C.; Saad, M. (2006): The 2D lid-driven cavity problem revisited. *Computers and Fluids*, vol. 35, pp. 326-348.

Buhmann, M. D. (2000): *Radial Basis Functions*. Cambridge University Press, Cambridge.

Chorin, A. (1967): A numerical method for solving incompressible viscous flow problems. *Journal of Computational Physics*, vol. 2, pp. 12-26.

Chorin, A. (1968): Numerical solution of the Navier-Stokes equations. *Mathematical Computation*, vol. 22, pp. 745-762.

De Vahl Davis, G. (1883): Natural convection of air in a square cavity: a benchmark numerical solution. *International Journal of Numerical Methods in Fluids*, vol. 3, pp. 249-264.

Divo, E.; Kassab, A. (2007): An efficient localized radial basis function meshless method for fluid flow and conjugate heat transfer. *Journal of Heat Transfer*, vol. 129, pp. 124-136.

Erturk, E. (2009): Discussions on driven cavity flow. *International Journal for Numerical Methods in Fluids*, vol. 60, pp. 275-294.

Erturk, E.; Corke, T.; Gökçöl, C. (2005): Numerical solutions of 2D steady incompressible driven cavity flow at high Reynolds numbers. *International Journal for Numerical Methods in Fluids*, vol. 48, pp. 747-774.

Erturk, E.; Gökçöl, C. (2006): Fourth-order compact formulation of Navier-Stokes equations and driven cavity flow at high Reynolds numbers. *International Journal for Numerical Methods in Fluids*, vol. 50, pp. 421-436.

Fasshauer, G.E. (2007): *Meshfree Approximation Methods with MATLAB*, Interdisciplinary Mathematical Sciences, vol. 6, World Scientific Publishers, Singapore.

Fluent, I. (2003): *FLUENT 6.1 User's Guide*. Lebanon (NH), Fluent Inc.

Franke, R. (1982): Scattered data interpolation: Tests of some methods. *Mathe-*

matics of Computation, vol. 38, pp. 181-200.

Ghia, U.; Ghia, K.; Shin, C. (1982): High-Re solutions for incompressible flow using the Navier-Stokes equations and a multigrid method. *Journal of Computational Physics*, vol. 48, pp. 387–411.

Gobin, D.; Le Quéré, P. (2000): Melting from an isothermal vertical wall, synthesis of a numerical comparison exercise. *Computer Assisted Mechanics and Engineerin Sciences*, vol. 198, pp. 289-306.

Grigoriev, M.; Dargush, G. (1999): A poly-region boundary element method for incompressible viscous fluid flows. *International Journal for Numerical Methods in Engineering*, vol. 46, pp. 1127–1158.

Gu, G.R.; Liu, Y. T. (2005): *An Introduction to Meshfree Methods and Their Programming*. Springer, Dordrecht.

Hon, Y.C.; Schaback R. (2001): On unsymmetric collocation by radial basis functions. *Applied Mathematics and Computation*, vol. 119, pp. 177-186.

Hou, S.; Zou, Q.; Chen, S.; Doolen, G.; and Cogley, A. C. (1995): Simulation of cavity flow by the lattice Boltzmann method. *Journal of Computational Physics*, vol. 118, pp. 329-347.

Kansa, E. (1990a): Multiquadrics: A scattered data approximation scheme with applications to computational fluid-dynamics I surface approximations and partial derivative estimates. *Computers and Mathematics with Applications*, vol. 19, pp. 127–145.

Kansa, E. (1990b): Multiquadrics: A scattered data approximation scheme with applications to computational fluid-dynamics II solutions to parabolic, hyperbolic and elliptic partial differential equations. *Computers and Mathematics with Applications*, vol. 19, pp. 147–161.

Kim, Y.; Kim, D.; Jun, S.; Lee, J. (2007): Meshfree point collocation method for the stream-vorticity formulation of 2D incompressible Navier–Stokes equations. *Computer Methods in Applied Mechanics and Engineering*, vol. 196, pp. 3095–3109.

Kosec, G.; Šarler, B. (2008a): Solution of thermo-fluid problems by collocation with local pressure correction. *International Journal of Numerical Methods for Heat and Fluid Flow*, vol. 18, pp. 868-882.

Kosec, G.; Šarler, B. (2008b): Local RBF collocation method for Darcy flow. *CMES: Computer Modeling in Engineering and Sciences*, vol. 25, pp. 197-208.

Kosec, G.; Šarler, B. (2009): Convection driven melting of anisotropic metals. *International Journal of Cast Metals Research*, vol. 22, pp. 279-282.

Kosec, G.; Šarler, B. (2010): Meshless approach to solving freezing with natural

convection. *Materials Science Forum*, vol. 649, pp. 205-210.

Kosec, G.; Šarler, B. (2011): H-adaptive local radial basis function collocation meshless method. *CMC: Computers Materials and Continua*, vol. 26, pp. 227-253.

Kosec, G.; Založnik, M.; Šarler, B.; Combeau, H. (2011): A meshless approach towards solution of macrosegregation phenomena. *CMC: Computers Materials and Continua*, vol. 22, pp. 169-196.

Kosec, G.; Šarler, B. (2013): Solution of a low Prandtl number natural convection benchmark by a local meshless method. *International Journal of Numerical Methods for Heat & Fluid Flow*, vol. 23, pp. 189-204.

Kovačević, I.; Šarler, B. (2005): Solution of a phase-field model for dissolution of primary particles in binary aluminum alloys by an r-adaptive mesh-free method. *Materials Science and Engineering*, vol. 413A, pp. 423-428.

Lee, C. K.; Liu, X.; Fan, S. C. (2003): Local multiquadric approximation for solving boundary value problems. *Computational Mechanics*, vol. 30, pp. 396-409.

Liao, S. (1992): Higher-order streamfunction-vorticity formulation of 2D steady-state Navier-Stokes equations. *International Journal for Numerical Methods in Fluids*, vol. 15, pp. 595-612.

Liao, S.; Zhu, J. (1996): A short note on high-order streamfunction-vorticity formulations of 2D steady state Navier-Stokes equations. *International Journal for Numerical Methods in Fluids*, vol. 22, pp. 1-9.

Lin, H.; Atluri, S.N. (2000): Meshless local Petrov-Galerkin (MLPG) method for convection-diffusion. *CMES: Computer Modeling in Engineering & Sciences*, vol.1. 45-60.

Lin, H.; Atluri, S. (2001): The meshless local Petrov-Galerkin (MLPG) method for solving incompressible Navier-Stokes equations. *CMES: Computer Modeling in Engineering and Sciences*, vol. 2, pp. 117-142.

Liu, G.R. (2010): *Meshfree methods. 2nd edition*. CRC Press, Boca Raton, FL.

Mramor, K.; Vertnik, R.; Šarler, B. (2013): Simulation of natural convection influenced by magnetic field with explicit local radial basis function collocation method. *CMES: Computer Modeling in Engineering & Sciences*, vol. 92, pp. 327-352.

Sahin, M.; Owens, R. (2003a): A novel fully implicit finite volume method applied to the lid-driven cavity problem. Part I: High Reynolds number flow calculations. *International Journal for Numerical Methods in Fluids*, vol. 42, pp. 57-77.

Sahin, M.; Owens, R. (2003b): A novel fully-implicit finite volume method ap-

plied to the lid-driven cavity problem. Part II: Linear stability analysis. *International Journal for Numerical Methods in Fluids*, vol. 42, pp. 79-88.

Šarler, B.; Perko, J.; Chen, C. S. (2004): Radial basis function collocation method solution of natural convection in porous media. *International Journal of Numerical Methods for Heat and Fluid Flow*, vol. 14, pp. 187-212.

Šarler, B. (2005): A radial basis function collocation approach in computational fluid dynamics. *CMES: Computer Methods in Engineering and Sciences*, vol. 7, pp. 185-193.

Šarler, B.; Vertnik, R. (2006): Meshfree explicit local radial basis function collocation method for diffusion problems. *Computers and Mathematics with Applications*, vol. 51, pp. 1269-1282.

Šarler, B.; Vertnik, R.; Mramor, K. (2012): A numerical benchmark test for continuous casting of steel. *IOP Conference Series: Materials Science and Engineering*, vol. 33., IOP Publishing. doi: 10.1088/1757-899X/33/1/012012.

Tolstykh, A.I.; Shirobokov D.A. (2003): On using radial basis functions in a “finite difference mode”. *Computational Mechanics*, vol. 33, pp. 68-79.

Vertnik, R.; Šarler, B. (2006): Meshless local radial basis function collocation method for convective-diffusive solid-liquid phase change problems. *International Journal of Numerical Methods for Heat and Fluid Flow*, vol. 16, pp. 617-640.

Vertnik, R.; Šarler, B. (2009): Solution of incompressible turbulent flow by a mesh-free method. *CMES: Computer Modeling in Engineering and Sciences*, vol. 44, pp. 65-96.

Vertnik, R.; Šarler, B. (2011): Local collocation approach for solving turbulent combined forced and natural convection problems. *Advances in Applied Mathematics and Mechanics*, vol. 3, pp. 259-279.

Wright; G.B; Fornberg, B. (2006): Scattered node compact finite difference-type formulas generated from radial basis function. *Journal of Computational Physics*, vol. 212, pp. 1623-1648.

Young, D.; Jane, S.; Fan, C.; Murugesan, K.; Tsai, C. (2006): The method of fundamental solutions for 2D and 3D Stokes problems. *Journal of Computational Physics*, vol. 211, pp. 1-8.

Zienkiewicz, O. C.; Codina, R. (1995): A general algorithm for compressible and incompressible flow - Part I. the split, characteristic-based scheme. *International Journal for Numerical Methods in Fluids*, vol. 20, pp. 869-885.

Zienkiewicz, O. C.; Morgan, K.; Sai, B. V. K.; Codina, R.; Vasquez, M. (1995): A general algorithm for compressible and incompressible flow - Part II. Tests on the explicit form. *International Journal for Numerical Methods in Fluids*, vol. 20, pp. 887-913.

